

# Electro-optically derived millimeter-wave sources with phase and amplitude control

Cite as: Appl. Phys. Lett. **119**, 151106 (2021); <https://doi.org/10.1063/5.0058815>

Submitted: 02 June 2021 • Accepted: 21 September 2021 • Published Online: 12 October 2021

Bryan T. Bosworth, Nick R. Jungwirth, Kassiopeia Smith, et al.

## COLLECTIONS

Paper published as part of the special topic on [Advances in 5G Physics, Materials, and Devices](#)



View Online



Export Citation



CrossMark

## ARTICLES YOU MAY BE INTERESTED IN

[Enhancing circular polarization of photoluminescence of two-dimensional Ruddlesden-Popper perovskites by constructing van der Waals heterostructures](#)

Applied Physics Letters **119**, 151101 (2021); <https://doi.org/10.1063/5.0062979>

[Demonstration of a compact x-ray free-electron laser using the optical klystron effect](#)

Applied Physics Letters **119**, 151102 (2021); <https://doi.org/10.1063/5.0064934>

[Probabilistic computing with p-bits](#)

Applied Physics Letters **119**, 150503 (2021); <https://doi.org/10.1063/5.0067927>

## Lock-in Amplifiers up to 600 MHz



Zurich  
Instruments



# Electro-optically derived millimeter-wave sources with phase and amplitude control

Cite as: Appl. Phys. Lett. **119**, 151106 (2021); doi: [10.1063/5.0058815](https://doi.org/10.1063/5.0058815)

Submitted: 2 June 2021 · Accepted: 21 September 2021 ·

Published Online: 12 October 2021





View Online



Export Citation



CrossMark

Bryan T. Bosworth,<sup>1</sup> Nick R. Jungwirth,<sup>1</sup> Kassiopeia Smith,<sup>1</sup> Jerome Cheron,<sup>1,2</sup>  Franklyn Quinlan,<sup>1</sup> Madison Woodson,<sup>3</sup>  Jesse Morgan,<sup>3</sup> Andreas Beling,<sup>3</sup> Ari Feldman,<sup>1</sup>  Dylan Williams,<sup>1</sup> Nathan D. Orloff,<sup>1,a)</sup>  and Christian J. Long<sup>1</sup>

## AFFILIATIONS

<sup>1</sup>National Institute of Standards and Technology, 325 Broadway Boulder, Colorado 80305, USA

<sup>2</sup>Department of Physics, University of Colorado, Boulder, Colorado 80302, USA

<sup>3</sup>Department of Electrical and Computer Engineering, University of Virginia, PO Box 400743, Charlottesville, Virginia 22904, USA

**Note:** This paper is part of the APL Special Collection on Advances in 5G Physics, Materials, and Devices.

<sup>a)</sup> Author to whom correspondence should be addressed: [orloff@nist.gov](mailto:orloff@nist.gov)

## ABSTRACT

Integrated circuits are building blocks in millimeter-wave handsets and base stations, requiring nonlinear characterization to optimize performance and energy efficiency. Today's sources use digital-to-analog converters to synthesize arbitrary electrical waveforms for nonlinear characterization, but this approach demands even faster integrated circuits to increase the bandwidth to millimeter-waves. Optically derived sources are a potential path to generate precise millimeter-waves and arbitrary waveforms using additive frequency synthesis. In this work, we demonstrate optically derived millimeter-waves up to 99.2 GHz with phase and amplitude control that could be locked to an optical reference. Our approach uses a 1550 nm electro-optic frequency comb with a terahertz of bandwidth. A programmable spectral filter selects two wavelengths from the optical comb, illuminating a modified uni-traveling carrier photodiode on a coplanar waveguide. We then tune the phase and amplitude by varying the optical phase and amplitude in the programmable spectral filter. The result of our work is electro-optically derived millimeter-waves at (24.8, 49.6, 74.4, and 99.2) GHz with phase and amplitude control, enabling arbitrary repetitive waveform generation.

Published by AIP Publishing. <https://doi.org/10.1063/5.0058815>

Optical frequency combs are sources of synchronized continuous wave (CW) optical lines with controllable spacing ( $f_{\text{rep}}$ ), ranging from the tens of MHz to tens of GHz.<sup>1</sup> Optical frequency combs can easily span several terahertz of bandwidth, and one can select any two lines via optical bandpass filtering to produce an optical beat with a frequency that is a multiple of  $f_{\text{rep}}$ . Earlier work by others demonstrated that uni-traveling carrier (UTC) photodiodes can downconvert the optical beat from an optical frequency comb to produce a millimeter-wave (mmWave, waves in the 30–300 GHz range) electrical signal at the beat frequency.<sup>2,3</sup>

The optical beat also inherits the phase stability of the comb. One recent example in the literature produced a 100 GHz electrical signal that had 70 dB lower phase noise than even the best electronic oscillators.<sup>4</sup> This significant improvement in phase noise might provide some advantages when characterizing mmWave integrated circuits, effectively eliminating uncertainties due to the source from the measurement and offering a new means to tailor measurement signals. For

instance, radar and communication systems require low phase noise performance for target estimation and receiver sensitivity, respectively. Ultra-low phase noise electronic signals are necessary to characterize precisely the system component performance, for example, the noise figure of amplifiers in new mmWave systems. Another advantage to optical synthesis of mmWaves is that a single comb can produce thousands of optical beat frequencies that are inherently synchronized with extremely low noise. Such complex optically derived signals<sup>5</sup> have the potential to facilitate new tests and measurements to understand nonlinearities and loss that impact the performance of mmWave technology.

Inspired by the literature,<sup>6</sup> we sought to test the generation of millimeter-waves with precise phase and amplitude control, taking a step toward optically derived arbitrary waveform generation by Fourier synthesis. Setting some goals for our experiment, we estimated that a Fourier series representation of a 25 GHz square wave with included harmonics up to 175 GHz would have a 10%–90% rise time

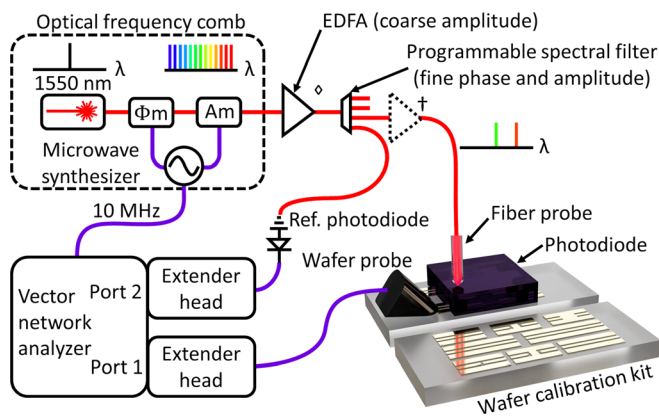


**FIG. 1.** Schematic of the electro-optically derived millimeter-wave source with phase and amplitude control. The optical frequency comb had 24.8 GHz spacing. A programmable spectral filter provided both fine phase and fine amplitude control. An erbium-doped fiber amplifier (EDFA) placed before (denoted  $\diamond$ ) or after (denoted  $\dagger$ ) the spectral filter provides coarse amplitude control. An on-wafer calibration sets the reference planes for the phase and amplitude measurements.

of 2.22 ps and an overshoot of 92.1 mV per 1 V peak-to-peak ( $V_{pp}$ ) amplitude. A Gaussian  $1\sigma$  uncertainty of 0.1 dB and 25 mrad on each of the odd harmonics of 25 GHz would increase these to only 2.24 ps  $\pm$  0.52 ps rise time and 104.0 mV  $\pm$  9.8 mV overshoot per 1 V  $V_{pp}$ . Thus, we set 0.1 dB and 25 mrad as our initial control goals.

In the following, we demonstrate electro-optically derived mmWaves with precise phase and amplitude control shown in Figs. 1 and supplementary material, Fig. S3. We begin by generating an optical frequency comb with a 24.8 GHz spacing. Then, we describe how to control phase and amplitude with a programmable spectral filter. We use a 110 GHz vector network analyzer (VNA) to measure an on-wafer modified UTC (MUTC) photodiode, operating in the linear range, and demonstrate our phase and amplitude control. Finally, we

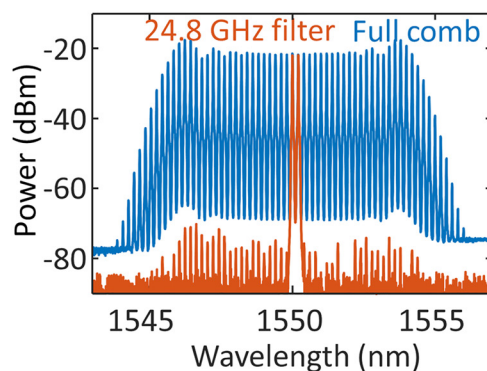
demonstrate arbitrary waveform synthesis using this phase and amplitude control and on-wafer measurement. Working on-wafer may allow us to extend this idea in future work well above 100 GHz, because the system is not limited by the coaxial connectors.

We generated an optical frequency comb via electro-optic phase and amplitude modulation of a narrow ( $<15$  kHz) linewidth CW fiber laser with an electrical sinewave at 24.8 GHz from a microwave synthesizer.<sup>7–9</sup> In practice, we connected a 25 GHz power amplifier to each of three electro-optic phase modulators to provide approximately 1 W of RF power per modulator. This electro-optic modulation resulted in greater than 1 THz of 3 dB optical bandwidth with a flat-top spectrum [Fig. 2(a)] that is a very good starting point for programmable phase and amplitude weighting of individual comb lines.

We chose 24.8 GHz comb spacing to place the fifth harmonic at 124 GHz, near the edge of the 110 GHz extender head maximum operating frequency. This 24.8 GHz choice gave us four tones in our measurement bandwidth at (24.8, 49.6, 74.4, and 99.2) GHz, which are within or near new proposed mmWave bands for 5G (24–28 GHz, 47–48 GHz, 66–71 GHz, and above 95 GHz).<sup>10,11</sup> However, the microwave calibration models (discussed in detail in the supplementary material) were not suitable to correct the data from 110 to 124 GHz. We attribute the issue to higher-order spatial modes in the coaxial cables and 1.0 mm connectors. For other applications, the fundamental comb spacing can be tuned continuously from below 1 GHz to the tens of GHz, which is limited by the bandwidth of the power amplifiers and electro-optic modulators.

We applied optical phase and amplitude control with a commercial programmable spectral filter (Finisar Waveshaper 4000<sup>24</sup>) based on a programmable liquid crystal on a silicon array at the Fourier plane of a diffraction grating.<sup>12</sup> The programmable spectral filter uses a two-dimensional (2D) liquid crystal array to direct optical wavelengths to one of four outputs with fine amplitude and phase control. Tuning the voltage waveform applied to the liquid crystal changes the index of refraction, resulting in an optical phase shift that is then converted to phase, amplitude, and output routing per wavelength.

### (a) Optical comb spectrum



### (b) Pulse autocorrelation

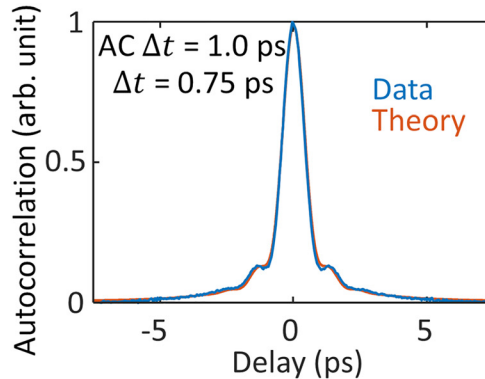


**FIG. 2.** The characteristics of the optical frequency comb in Fig. 1 configuration  $\dagger$ . The electro-optically generated comb has a flat-top spectrum shown before the EDFA (a, Full comb) that undergoes linear amplitude and phase shifts in the programmable spectral filter. Unused spectral lines are rejected by  $>50$  dB outside the passband [(a), 24.8 GHz filter]. For arbitrary waveform generation, the optical pulses are almost fully compressed to create a flat spectral phase that can be seen in the intensity autocorrelation (b). The theory curve in (b) represents the autocorrelation of the pulse from a simulated optical frequency comb with its calculated spectrum fit to the measured comb spectrum and its spectral phase up to fourth polynomial order removed. Autocorrelation (AC) and pulse full width at half maximum durations are shown in (b).

For the two outputs in these measurements, we selected pairs of comb lines as close as possible to the CW laser wavelength to minimize the effect of noise added during the optical comb generation. Arbitrary filter profiles can be programmed with passband widths from 10 GHz to greater than 5 THz and a frequency resolution of 1 GHz. Linear attenuation and phase shift is discussed below; unwanted wavelengths can be blocked by more than 50 dB, which is depicted for a 24.8 GHz filter profile in Fig. 2(a). In general, liquid crystal programmable spectral filters can refresh the full filter profile up to several hundred Hz, but the commercial filter is software limited to approximately 1 Hz. For higher speed and potentially higher precision, a wavelength demultiplex and remultiplex is straightforward to implement with a modulator in between. In this case, amplitude and phase shifting can be accomplished with electro-optic modulators, MEMs, fiber stretching, etc., at the expense of complexity and more need to stabilize the different mmWave frequencies' phases against drift.

Because the pulses from electro-optic comb generation are strongly chirped (20 ps duration), we corrected the spectral phase in the programmable spectral filter up to the fourth polynomial order ( $\beta_2, \beta_3, \beta_4$ ). In Fig. 2(b), we compare the compressed pulse autocorrelation at the plane of the fiber probe (Fig. 1, configuration †) against a theoretical pulse derived from fitting the comb generation parameters (modulation index, bias, etc.) to the measured optical spectrum [Fig. 2(a)]. The agreement between the theory and experiment indicates that the pulses were nearly transform-limited, i.e., a very good starting point for the arbitrary waveform generation is discussed below.

Precise measurement of optical phase control meant we required a stable phase reference. The 10 MHz reference from the microwave synthesizer (Fig. 1) aligned the frequency grid of the VNA to the optical frequency comb spacing. Unfortunately, the local oscillator inside our VNA, which mixes the measured electrical signal down to the VNA's internal intermediate frequency (IF), adds a random phase offset. We, therefore, attached a 1.0 mm connectorized 100 GHz photodiode (Finisar) to the VNA port 2 to act as the phase reference. This packaged reference photodiode used an optical fiber input, whereas a cleaved fiber probe illuminated the MUTC photodiode (discussed below). To measure the phase at a multiple of 24.8 GHz, we directed a separate pair of comb lines to the second port of the spectral filter and out to the phase reference photodiode. We subtracted the reference phase from the measured phase of the on-wafer photodiode as we swept the coarse amplitude or fine phase and amplitude through the range of interest. The phase reference provided a constant phase signal synchronized to the optical frequency comb as we optically tuned the amplitude or phase of the beat input to the on-wafer photodiode. We did not need the reference photodiode to act as a comb generator with characterized phase response across frequencies, because we were primarily concerned with the linearity and control resolution of the programmable spectral filter and on-wafer photodiode together. Future work will explore the benefits of a reference photodiode traceable to the NIST electro-optic sampling system.<sup>13–16</sup>

The MUTC photodiode is a double-mesa InGaAsP/InP photodiode with 8  $\mu\text{m}$  diameter; the device is flip-chip bonded onto an aluminum nitride substrate for heat sinking with gold coplanar waveguide (CPW) contacts. This type of photodiode has been previously demonstrated to have 3 dB bandwidths larger than 100 GHz, high linearity, and high output power.<sup>3,17,18</sup> Because we want to create arbitrary

waveforms at low mmWave frequencies as well as frequencies beyond the second mode cutoff of current coaxial connectors (110 GHz for 1.0 mm connectors and 145 GHz for 0.8 mm connectors), we measured the photodiode on-wafer with a CPW output rather than bonding it to a coaxial connector. mmWaves above 100 GHz presented here will be measured with different extender heads and on-wafer probes in the future.

To verify the performance of the photodetector as a precision wideband mmWave source, we removed the unwanted effects of the cables and wafer probes by performing a two-tier microwave calibration and a power calibration. The VNA commonly measures scattering parameters (S-parameters) of networks with internal sources and receivers. For these measurements, we wanted to know phase and amplitude of externally generated mmWaves. To do this, we measured the uncorrected outgoing ( $a_1, a_2$ ) and returned ( $b_1, b_2$ ) raw voltage wave parameters and corrected them outside of the VNA firmware. We recorded all eight wave parameters (four with the VNA source exciting port 1 and port 2 alone in succession) for each device required in the microwave calibration. Measuring both the wave-parameters and the power calibration with the power standard let us characterize the absolute power of the fundamental and harmonic content of the MUTC photodiode. We consider the power calibration and on-wafer calibrations essential to the characterization of MUTC photodiodes as precision mmWave sources and describe them in detail in the [supplementary material](#).<sup>14,19–23</sup>

After taking all the data required to calibrate our measurements, we applied light to the photodiode and recorded the outgoing ( $a_1, a_2$ ) and returned ( $b_1, b_2$ ) raw voltage wave parameters in the VNA with the internal sources turned off. Next, we multiplied the vectors of  $a$  and  $b$  wave parameters by the translated VNA calibration matrices to compute the desired  $a$  and  $b$  waves at the edge of the photodiode. Finally, this correction produced the outgoing  $b$  wave from the edge of the photodiode, which is the corrected measurement of phase and amplitude of the optically generated mmWaves.

Of course, photodiodes designed for mmWave frequencies are nonlinear devices under large optical input power (i.e., several mW). One of the most common ways of investigating a device's linear operating range is to increase the input optical power until it reaches saturation.<sup>17</sup> In saturation, the output electrical power starts to hit a maximum, and the input to output power conversion slope falls well below a positive linear response or even becomes negative (Fig. 3).

We investigated the linear range of our photodiode by moving the EDFA after the programmable spectral filter (position † in Fig. 1). Placing the EDFA last protects the programmable filter from the required powers above 100 mW for two comb lines. (The power delivered to the active region of the photodiode was lower because of bending loss in the fiber probe and diffraction from the cleaved fiber tip.) We increased the optical power at the photodiode using the pump current to the second stage power amplifier inside the EDFA. The EDFA gain spectrum naturally changed with increasing pump power. To compensate, we set the programmable spectral filter to equalize the two selected comb lines using the traces from an optical spectrum analyzer.

For each mmWave frequency of interest, we selected and equalized two comb lines in the filter and increased the optical power until the photodiode reached saturation. To prevent any photodiode damage at very high optical input powers, we chose to do fewer tests at



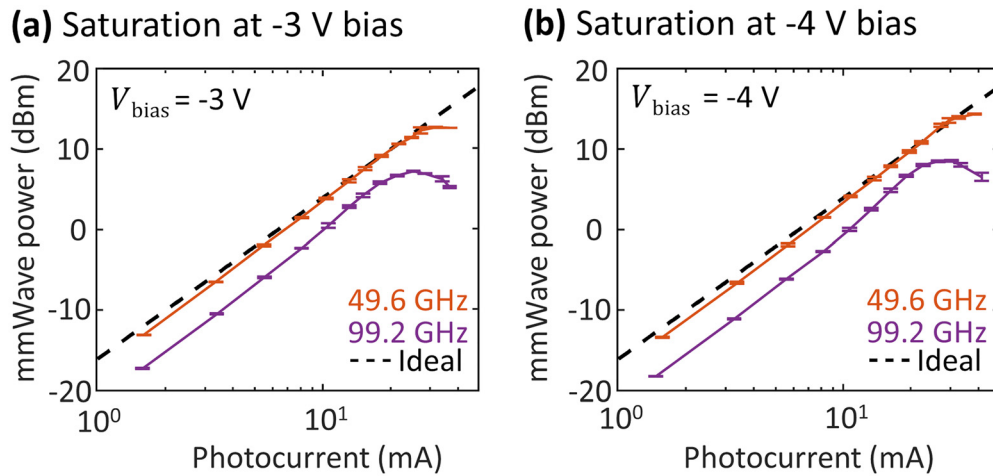


**FIG. 3.** The photodiode saturation behavior at  $V_{\text{bias}} = -3 \text{ V}$  (a) and  $V_{\text{bias}} = -4 \text{ V}$  (b) between the center conductor of the coplanar waveguide and ground planes. As photocurrent (optical power) increases, the output power of the mmWave increases until the photodiode saturates. Only 49.6 GHz (red) and 99.2 GHz (purple) are shown, because the measurement can damage the photodiode. Uncertainties in millimeter-wave power based on a 68% confidence interval.

49.6 and 99.2 GHz and bias voltages of  $-3$  and  $-4 \text{ V}$ . For both bias voltages, the output 99.2 GHz power peaks at 25–30 mA photocurrent.

Setting the programmable spectral filter to add attenuation or phase shift to one of the two comb lines allowed for fine phase and amplitude control. We tested this approach in nominal steps of 25 mrad and 0.1 dB (Fig. 4), which we uploaded as profiles in the spectral filter software. The EDFA was installed in position  $\diamond$  in Fig. 1 to avoid nonuniform gain vs wavelength during the fine control measurement. Because we wanted to avoid photodiode saturation completely, we set the average photocurrent to 0.1 mA before attenuation. The horizontal axis in Fig. 4 represents the nominal value applied in the spectral filter profile, and the response was very linear. At 24.8 GHz, we found the highest attenuation slope in Fig. 4(a). This high attenuation was likely

due to the crosstalk between adjacent bands in the programmable spectral filter. There also appeared to be some drift in the measured fine amplitude and phase control, which was most noticeable in the phase control at 74.4 GHz. For this experiment, we did not control the bias of the electro-optic amplitude modulator, and slow drift over several minutes in the ideal bias voltage may have created the random walk apparent in the data. The phase drift could also be due, in part, to the few meters of fibers that were not common between the reference and MUTC photodiodes.

After demonstrating that we could generate mmWaves with fine, linear phase and amplitude control, we created a proof-of-concept arbitrary waveform generator. We changed the setup in Fig. 1 by connecting the output of the wafer probe to a 100 GHz sampling

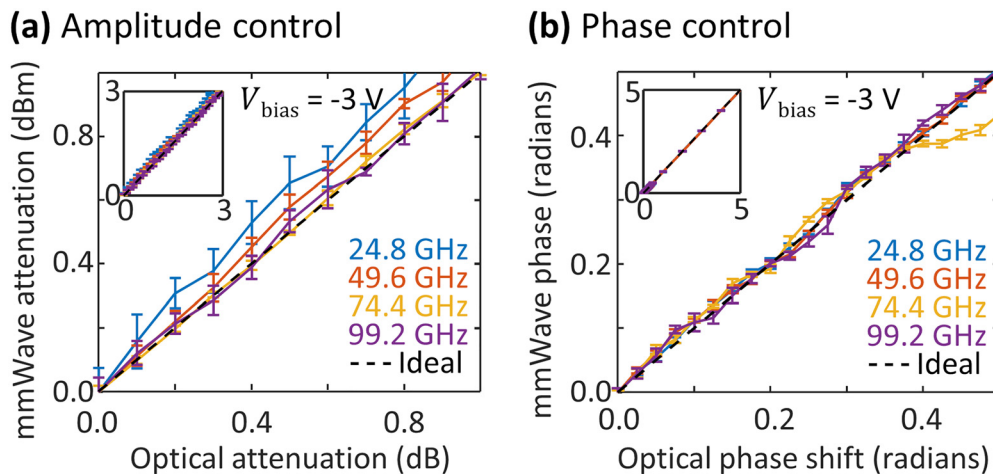


**FIG. 4.** (a) Millimeter-wave attenuation vs optical attenuation for sinusoidal electrical waves at 24.8 GHz (blue line), 49.6 GHz (red line), 74.4 GHz (yellow line), 99.2 GHz (purple line), and the ideal line (black dashed). (b) Millimeter-wave phase vs optical phase for sinusoidal electrical waves at 24.8 GHz (blue line), 49.6 GHz (red line), 74.4 GHz (yellow line), 99.2 GHz (purple line), and the ideal line (black dashed). Uncertainties in millimeter-wave attenuation and phase based on a 68% confidence interval. Insets show coarse amplitude and phase control over 3 dB and 5 rad.

oscilloscope rather than the VNA. Then, we used the measured impulse response [Fig. 5(a)] to compute the necessary predistortion for waveforms measured at the reference plane of the sampler in the oscilloscope. In the same step, we optimized the phase and amplitude coefficients of five comb lines into a simulated ideal photodiode to generate four different arbitrary waveforms [Figs. 5(b)–5(e)]. For these experiments, the photocurrent had a DC level of 7.5 mA at  $-3$  V bias, which generated large amplitude signals slightly below the onset of nonlinearities above 10 mA [Fig. 3(a)]. For all waveforms, the waveform coefficients included extra phase correction to compress the pulses [Fig. 2(b)] and amplitude correction to equalize the comb lines (including the EDFA gain). The predicted waveforms including the effect of the impulse response (denoted “theory” in Fig. 5) and the measured waveforms show excellent agreement. However, the measured waveforms often show a small amount of tilt or overshoot due to imperfect comb line equalization, which can be addressed in our future studies that will expand the bandwidth of the waveforms and move the reference plane on-wafer to the edge of the photodiode.

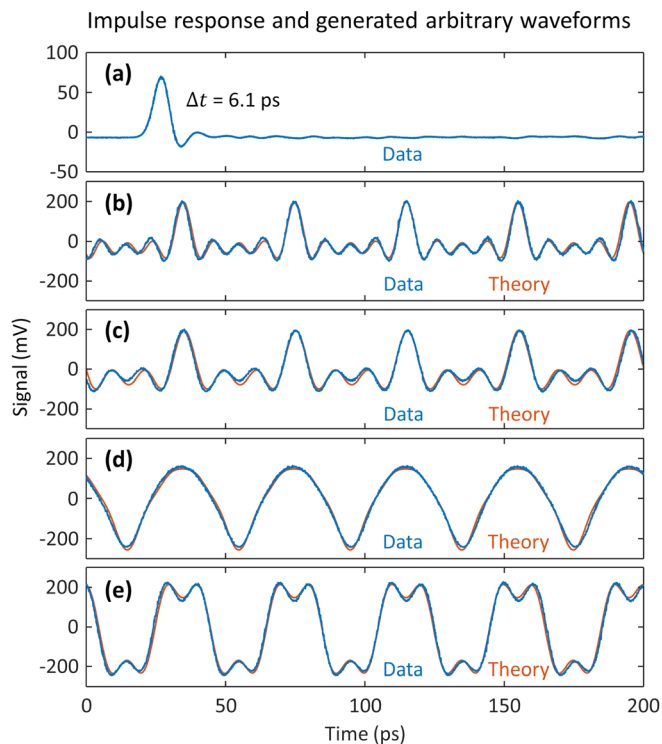


**FIG. 5.** Sampling oscilloscope measurements of the impulse response of the on-wafer photodiode and several generated waveforms. A computer program optimized the amplitude and phase coefficients of five central optical frequency comb lines to match several desired shapes after simulated photodetection. (a) The linear impulse response (a full width at half maximum duration of 6.1 ps) was used in the optimization to predistort the optical signal to yield the desired electrical waveform at the sampler in the oscilloscope. Theory (b)–(e) curves denote the predicted waveforms after photodetection. The waveforms have 24.8 GHz repetition frequency and up to 100 GHz bandwidth: (b) sinc pulses with 100 GHz of bandwidth, (c) sinc pulses with 75 GHz of bandwidth, (d) rectified sine waves, and (e) square waves.

In this paper, we synthesized electro-optically derived millimeter-waves with phase and amplitude control and generated arbitrary repetitive waveforms, which avoid the challenges for ultrabroadband time-domain arbitrary waveform generation. To test our approach, we built a 1550 nm optical frequency comb with over a terahertz of bandwidth. We used a programmable spectral filter to select and control two optical comb lines. A photodiode downconverted the optical beat producing a millimeter-wave at the envelope frequency, which we used to synthesize millimeter-waves at (24.8, 49.6, 74.4, and 99.2) GHz. The key idea was to use the optical domain to control the optical phase and amplitude, which, in turn, controlled the phase and amplitude of the millimeter-wave in the electronic domain. As a result, we controlled the electronic phase in 25 mrad steps and the electronic amplitude in 0.1 dB steps. Future work could improve phase noise by stabilizing the optical frequency comb, which is discussed along with other ways to make this experiment better in the [supplementary material](#). To summarize, this work demonstrated electro-optically derived millimeter-waves and arbitrary waveforms with precise phase and amplitude control.

See the [supplementary material](#) for discussion of on-wafer calibration, mmWave harmonic content, and noise performance.

The authors thank the critical review of Dr. T. Mitchell Wallis, Dr. Nikunj Kumar Prajapati, Dr. James C. Booth, and Dr. Paul D. Hale. The National Institute of Standards and Technology funded this work as an Innovations in Measurement Science Grant. Dr. Bosworth, Dr. Jungwirth, and Dr. Smith thank the National Research Council for sponsoring their postdoctoral fellowships. Dr. Orloff thanks valuable conversations with Dr. M. Jarahi of University of California Los Angeles, Dr. M. Shimizu, and Dr. T. Ishibashi of NTT.

This paper is an official contribution of NIST; it is not subject to copyright in the U.S. Usage of commercial products herein is for information only; it does not imply recommendation or endorsement by NIST; other products may work as well or better.

#### DATA AVAILABILITY

The data that support the findings of this study are available from the corresponding author upon reasonable request.

#### REFERENCES

- <sup>1</sup>T. Fortier and E. Baumann, “20 years of developments in optical frequency comb technology and applications,” *Commun. Phys.* **2**, 153 (2019).
- <sup>2</sup>T. Ishibashi, Y. Muramoto, T. Yoshimatsu, and H. Ito, “Unitraveling-carrier photodiodes for terahertz applications,” *IEEE J. Sel. Top. Quantum Electron.* **20**, 3804210 (2014).
- <sup>3</sup>Z. Li, Y. Fu, M. Piels, H. Pan, A. Beling, J. E. Bowers, and J. C. Campbell, “High-power high-linearity flip-chip bonded modified uni-traveling carrier photodiode,” *Opt. Express* **19**, B385 (2011).
- <sup>4</sup>T. M. Fortier, A. Rolland, F. Quinlan, F. N. Baynes, A. J. Metcalf, A. Hati, A. D. Ludlow, N. Hinkley, M. Shimizu, T. Ishibashi, J. C. Campbell, and S. A. Diddams, “Optically referenced broadband electronic synthesizer with 15 digits of resolution,” *Laser Photonics Rev.* **10**, 780–790 (2016).
- <sup>5</sup>A. M. Weiner, “Manipulation of ultrashort pulses,” in *Ultrafast Optics* (John Wiley & Sons, Inc., 2009), pp. 362–421.
- <sup>6</sup>V. Torres-Company and A. M. Weiner, “Optical frequency comb technology for ultra-broadband radio-frequency photonics,” *Laser Photonics Rev.* **8**, 368–393 (2014).

- <sup>7</sup>A. J. Metcalf, V. Torres-Company, D. E. Leaird, and A. M. Weiner, "High-power broadly tunable electrooptic frequency comb generator," *IEEE J. Sel. Top. Quantum Electron.* **19**, 3500306 (2013).
- <sup>8</sup>T. Yamamoto, T. Komukai, K. Suzuki, and A. Takada, "Multicarrier light source with flattened spectrum using phase modulators and dispersion medium," *J. Light. Technol.* **27**, 4297–4305 (2009).
- <sup>9</sup>V. Torres-Company, J. Lancis, and P. Andrés, "Lossless equalization of frequency combs," *Opt. Lett.* **33**, 1822 (2008).
- <sup>10</sup>ETSI 3rd Generation Partnership Project (3GPP), "5G; NR; User Equipment (UE) radio transmission and reception; Part 1: Range 1 Standalone," 3GPP TS 138.101-1 version 15.3.0 (2018).
- <sup>11</sup>T. S. Rappaport, Y. Xing, O. Kanhere, S. Ju, A. Madanayake, S. Mandal, A. Alkhateeb, and G. C. Trichopoulos, "Wireless communications and applications above 100 GHz: Opportunities and challenges for 6G and beyond," *IEEE Access* **7**, 78729–78757 (2019).
- <sup>12</sup>A. M. Weiner, "Ultrafast optical pulse shaping: A tutorial review," *Opt. Commun.* **284**, 3669–3692 (2011).
- <sup>13</sup>T. Albrecht, J. Martens, T. S. Clement, P. D. Hale, and D. F. Williams, "Broadband characterization of optoelectronic components to 65 GHz using VNA techniques," in *ARFTG Conference* (IEEE, 2003), pp. 53–59.
- <sup>14</sup>P. D. Hale and D. F. Williams, "Calibrated measurement of optoelectronic frequency response," *IEEE Trans. Microwave Theory Tech.* **51**, 1422–1429 (2003).
- <sup>15</sup>Anritsu Company, *Electro-Optical Measurements using Anritsu VNAs* (Anritsu Company, 2020).
- <sup>16</sup>Anritsu Company, *O/E Calibration Module MN4765B Data Sheet* (Anritsu Company, 2020).
- <sup>17</sup>Q. Li, K. Li, Y. Fu, X. Xie, Z. Yang, A. Beling, and J. C. Campbell, "High-power flip-chip bonded photodiode with 110 GHz bandwidth," *J. Light. Technol.* **34**, 2139–2144 (2016).
- <sup>18</sup>A. Beling, X. Xie, and J. C. Campbell, "High-power, high-linearity photodiodes," *Optica* **3**, 328 (2016).
- <sup>19</sup>National Institute of Standards and Technology, <http://www.nist.gov/services-resources/software/wafer-calibration-software> for "NIST Microwave Uncertainty Framework" (2011).
- <sup>20</sup>J. Verspecht, "Calibration of a measurement system for high frequency nonlinear devices," Ph.D. dissertation (Vrije Universiteit Brussel, 1995).
- <sup>21</sup>N. D. Orloff, J. Mateu, A. Lewandowski, E. Rocas, J. King, D. Gu, X. Lu, C. Collado, I. Takeuchi, and J. C. Booth, "A compact variable-temperature broadband series-resistor calibration," *IEEE Trans. Microwave Theory Tech.* **59**, 188–195 (2011).
- <sup>22</sup>D. C. DeGroot, J. A. Jargon, and R. B. Marks, "Multiline TRL revealed," in *60th ARFTG Conference Digest, Fall 2002* (IEEE, 2002), pp. 131–155.
- <sup>23</sup>R. B. Marks, "A multiline method of network analyzer calibration," *IEEE Trans. Microwave Theory Tech.* **39**, 1205–1215 (1991).
- <sup>24</sup>Certain commercial equipment, instruments, or materials are identified in this paper in order to specify the experimental procedure adequately. Such identification is not intended to imply recommendation or endorsement by the National Institute of Standards and Technology, nor is it intended to imply that the materials or equipment identified are necessarily the best available for the purpose.